Scattering from a Large Body with Cracks and Cavities by the Fast and Accurate Finite-Element Boundary-Integral Method

Xin-Qing Sheng, Edward Kai-Ning Yung, Chi H. Chan, J. M. Jin, and W. C. Chew

***Abstract*—A large body with cracks and cavities is a kind of typical structure widely existing in realistic targets. In this paper, a newly developed fast and accurate finite-element boundary-integral (FA-FE-BI) method is applied to compute scattering by this kind of scatterers. A thorough analysis on this FA-FE-BI numerical technique is presented, clearly demonstrating that this technique has computational complexity $O(N \log N)$ and memory requirement $O(N)$ (N is the total number of surface unknowns). An inward-looking approach is employed as a preconditioner to speed up the rate of convergence of iterative solvers for this structure. Under these techniques, a powerful code is developed for this kind of scatterers whose accuracy, efficiency, and capability is well confirmed by various numerical results.**

***Index Terms*—Electromagnetic scattering, finite-element boundary-integral method, multilevel fact multipole algorithm.**

I. INTRODUCTION

THE calculation of scattering by a large body with cracks and cavities has been of considerable interests because cracks and cavities widely exist in realistic targets and often they are dominant contributors to the scattering behavior of targets. Various empirical analytical methods have been developed to analyze this kind of problem such as the geometrical theory of diffraction (GTD) solution for wide cracks [1], the low-frequency approximation solution for narrow cracks [2], and the solution based on the two types of scattering mechanisms for the cracks having large contours [3]. However, all of these analytical methods are designed for specific problems. Furthermore, good results from these methods often rely on the deep physical understanding to the problem.

As computers grow faster and faster, more engineering and scientific problems are solved with numerical techniques. Over the past, an efficient low-frequency technique, hybrid finite-element boundary-integral (FE-BI) method, has been developed to calculate scattering from cavities in an infinite ground plane [4]–[6], but it cannot include the effect of arbitrarily shaped large bodies. To include all effects of a large body, small features, and their interactions, an innovative hybrid scheme of the shooting-and-bouncing-ray (SBR) and the finite-element method (FEM) has been proposed to calculate electromagnetic scattering by some realistic targets [7], [8]. In this hybrid scheme, one needs to calculate the scattering of the incident wave by a large body without small features, which can be efficiently computed with the SBR and the scattering of equivalent magnetic current by the large body without small features, which is approximated as scattering of equivalent magnetic current by an infinite conducting plane. This approximation is available only for cracks existing on the flat surface and far away from the reflecting surface, which is not true for some realistic targets.

Eliminating the restriction of the method in [7] by the fast and accurate FE-BI method [9] is the goal of this paper. In this paper, we first employ the efficient and accurate FE-BI method to formulate the problem of scattering by a large body with cracks and cavities. Then we apply the multilevel fast multipole algorithm (MLFMA) to the boundary integral equation (BIE) to significantly reduce the memory requirement and computational time. A thorough analysis of the cost of this technique clearly demonstrates that it has computational complexity $O(N \log N)$ and memory requirement $O(N)$ (N denotes the number of surface unknowns of the large body). To speed up the rate of convergence of the conjugate gradient (CG) method, an inward-looking approach [10] is then employed as a preconditioner to improve the spectral property of the final FE-BI matrix equation. Various numerical results, and the choices of parameters and interpolation (or anterpolation) technique in the MLFMA are given in Section IV, demonstrating that the scattering of a large body with cracks and cavities can be generally, accurately, and efficiently computed by this technique.

II. FORMULATION

Consider the problem of electromagnetic wave scattering by a large body with cracks and cavities, whose cross section is illustrated in Fig. 1. The cracks and cavities can be empty or filled with inhomogeneous materials characterized by relative permittivity and permeability (ϵ_r, μ_r). Owing to the cracks and cavities on the curved surface and close to the reflecting surface, there are strong and complex interactions between small features and the large body and it is difficult to decouple the original problem into two separate problems as in [7]. Therefore, we have to consider the small features and the large body as a whole. To this end, we employ the newly developed efficient and accurate FE-BI formulation [9] to formulate this kind of specific problem.

Manuscript received January 18, 1999; revised May 2, 2000.

X.-Q. Sheng, E. K.-N. Yung, and C. H. Chan are with the Department of Electronic Engineering, City University of Hong Kong, Hong Kong (e-mail: eexsheng@cityu.edu.hk).

J. M. Jin and W. C. Chew are with the Center for Computational Electromagnetics, Department of Electrical and Computer Engineering, University of Illinois at Urbana-Champaign, Urbana, IL 61801-2991 USA.

Publisher Item Identifier S 0018-926X(00)06933-7.

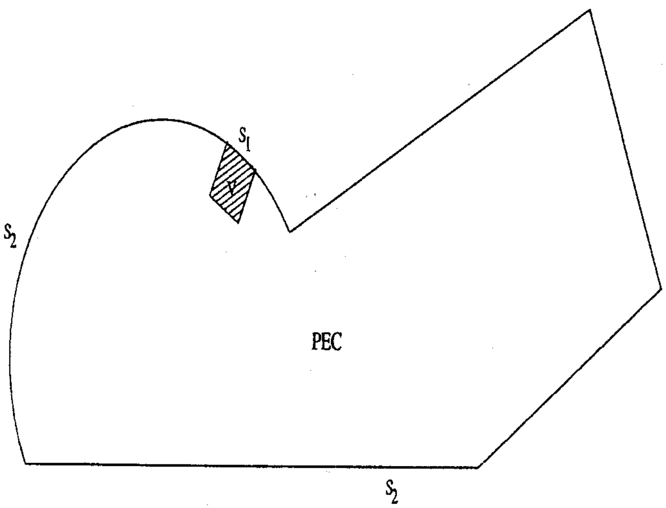

Fig. 1. A large arbitrarily shaped body with a small cavity.

The field in the interior region can be formulated into an equivalent variational problem with the functional given by [11]

$$F(\mathbf{E}) = \frac{1}{2}\int_V \left[\frac{1}{\mu_r}(\nabla\times\mathbf{E})\cdot(\nabla\times\mathbf{E}) - k_0^2\epsilon_r\mathbf{E}\cdot\mathbf{E}\right]dV + jk_0\int_{S_1}(\mathbf{E}\times\overline{\mathbf{H}})\cdot\hat{n}\,dS \quad (1)$$

where

V	interior volume of the cavity;
S_1	outside part of the surface of the cavity through which the interior field in the cavity interacts with the exterior field;
$\hat{n}$	outward unit normal to S_1;
k_0	free-space wavenumber;
$\overline{\mathbf{H}} = Z_0\mathbf{H}$ with Z_0	free-space intrinsic impedance.

Using the FEM with tetrahedral edge elements, we obtain the matrix equation

$$\begin{bmatrix} K_{II} & K_{IS} & 0 \\ K_{SI} & K_{SS} & B_1 \end{bmatrix}\begin{Bmatrix} E_I \\ E_{S_1} \\ \overline{H}_{S_1} \end{Bmatrix} = \begin{Bmatrix} 0 \\ 0 \end{Bmatrix} \quad (2)$$

where $\{E_I\}$ is a vector containing the discretized electric field inside V, $\{E_{S_1}\}$, and $\{\overline{H}_{S_1}\}$ are the vectors containing the discretized electric and magnetic fields on S_1, respectively. Furthermore, $[K_{II}]$, $[K_{IS}]$, $[K_{SI}]$, $[K_{SS}]$, and $[B_1]$ are sparse submatrices and, in particular, $[K_{II}]$ and $[K_{SS}]$ are symmetric, $[B_1]$ is skew symmetric and $[K_{IS}] = [K_{SI}]^T$, where the superscript T denotes a transpose operation.

Equation (2) cannot be solved unless a relation between $\{E_{S_1}\}$ and $\{\overline{H}_{S_1}\}$ is established. In [9] such a relation is directly provided by the boundary integral equation. However, the surface region S_1 in this problem is only the part of the large body surface, hence, the integral equation cannot be used in the surface region S_1. To overcome this difficulty, we introduce another equivalent electric current on the surface region S_2 (S_2 denotes the surface region of the large body except S_1), thus, the relation between $\{E_{S_1}\}$ and $\{\overline{H}_{S_1}\}$ can be obtained with the aid of J_2 on the surface region S_2. Applying the electric-field integral equation (EFIE) to the exterior region outside S_1 and S_2

$$\mathbf{L}_1(\overline{\mathbf{J}}_1) - \mathbf{K}_1(\mathbf{M}_1) + \mathbf{L}_2(\overline{\mathbf{J}}_2) = \mathbf{E}^i \quad (3)$$

is obtained. Applying the magnetic field integral equation (MFIE) to the exterior region

$$\mathbf{K}_1(\overline{\mathbf{J}}_1) + \mathbf{L}_1(\mathbf{M}_1) + \mathbf{K}_2(\overline{\mathbf{J}}_2) = \overline{\mathbf{H}}^i \quad (4)$$

is also obtained, where $\mathbf{L}_i$ and $\mathbf{K}_i$ are the integro-differential operators [9], $\overline{\mathbf{J}}_1$, $\overline{\mathbf{J}}_2$ and $\mathbf{M}_1$ are related to the fields on S by $\mathbf{J}_1 = \hat{n}\times\overline{\mathbf{H}}_1$, $\mathbf{J}_2 = \hat{n}\times\overline{\mathbf{H}}_2$ and $\mathbf{M}_1 = \mathbf{E}_1\times\hat{n}$, respectively, and ($\mathbf{E}^i$, $\mathbf{H}^i$) denote the incident fields.

Similar to [9], we employ the following linear combination of EFIE, $\hat{n}\times$ EFIE, and $\hat{n}\times$ MFIE

$$\begin{aligned}(\mathbf{L}_1 + \hat{n}\times\mathbf{L}_1 - \hat{n}\times\mathbf{K}_1)\,(\overline{\mathbf{J}}_1) \\ + (\mathbf{K}_1 + \hat{n}\times\mathbf{K}_1 + \hat{n}\times\mathbf{L}_1)(\mathbf{M}_1) \\ + (\mathbf{L}_2 + \hat{n}\times\mathbf{L}_2 - \hat{n}\times\mathbf{K}_2)\,(\overline{\mathbf{J}}_2) \\ = \mathbf{E}^i + \hat{n}\times\mathbf{E}^i + \hat{n}\times\overline{\mathbf{H}}^i\end{aligned} \quad (5)$$

as the exterior equation to obtain good accuracy and efficiency, and eliminate the problem of interior resonance. Discretizing (5) yields

$$[P]\{E_{S_1}\} + [Q]\{\overline{H}_S\} = \{b\} \quad (6)$$

where $\{\overline{H}_S\}$ denotes $\{\overline{H}_{S_1}\overline{H}_{S_2}\}^T$.

Combining (2) and (6), we obtain the complete system

$$\begin{bmatrix} K_{II} & K_{IS} & 0 \\ K_{SI} & K_{SS} & B \\ 0 & P & Q \end{bmatrix}\begin{Bmatrix} E_I \\ E_{S_1} \\ \overline{H}_S \end{Bmatrix} = \begin{Bmatrix} 0 \\ 0 \\ b \end{Bmatrix} \quad (7)$$

which can be solved for the field inside V and on S_1, S_2.

For large targets having a large number of unknowns in (7), it becomes more expedient to choose iterative methods to solve (7) since the computational complexity and memory requirement of iteratives methods are less than those of direct methods. It is well known that the dominant CPU time for iterative methods is the product of two factors: the time for each iteration and the number of iteration required for a convergent solution. The first factor can be significantly reduced by the MLFMA, which will be detailed in the next section. The second factor usually depends on spectral properties of the matrix that ultimately are controlled by the geometry of the problem. For the specific geometry structure of a large body with cracks and cavities discussed in this paper, the small features often distort the spectral distribution of the matrix in (7) resulting in a slow convergence. To improve the spectral property of (7), a preconditititioner similar to the inward-looking approach [10] is employed. The expression of the interior unknowns $\{E_i\}$ in the cracks with the surface unknowns of the cracks $\{E_{S_1}\}$ is first obtained using a direct method

$$\{E_I\} = -[K_{II}]^{-1}[K_{IS}]\{E_{S_1}\}. \tag{8}$$

Since the number of the interior unknowns in a crack is typically small, the CPU time for (8) can be omitted compared with that for solving the whole equation. Furthermore, this step is computed only once for all excitations. Substituting (8) into (7) yields the final equation

$$\begin{bmatrix} K'_{SS} & B \\ P & Q \end{bmatrix} \begin{Bmatrix} E_{S_1} \\ \overline{H}_S \end{Bmatrix} = \begin{Bmatrix} 0 \\ b \end{Bmatrix} \tag{9}$$

which has a more favorable spectral property. Here, submatrix $[K'_{SS}]$ is given by

$$[K'_{SS}] = [K_{SS}] - [K_{SI}]\,[K_{II}]^{-1}[K_{IS}]. \tag{10}$$

III. Application and Analysis of the MLFMA

Since the number of unknowns in $\{E_{S_1}\}$ is very small compared with that in $\{H_S\}$, the CPU time for the whole matrix-vector multiplication is mainly governed by the multiplication of matrix $[Q]$ and vector $\{H_S\}$. Also, the memory requirement is dominated by the dense matrix $[Q]$. The computational complexity and memory requirement in the multiplication of $[Q]$ and $\{H_S\}$ can be significantly reduced by the MLFMA.

To detail the implementation and demonstrate the computational complexity and memory requirement of the MLFMA, consider a special case without loss of generality of the MLFMA, where the integral surface is a square plane. The square is first divided into four smaller squares illustrated in Fig. 2(a), named as "level 1." The symbol "$*$" in Fig. 2(a) denotes the center of each subsquare. Each subsquare is then recursively subdivided into smaller squares until the edge length of the finest square is about half of a wavelength. Here, we just consider a three-level MLFMA. Fig. 2(b) and (c), respectively, illustrate the situation of level 2 and level 3, where the symbols "o" and "$\cdot$" stand for the center of each subsquare in level 2 and level 3, respectively.

In the MLFMA, the matrix–vector multiplication is considered to be the interaction of radiation sources, which is accomplished through three processes: 1) the aggregation process; 2) the translation process; and 3) the disaggregation process. The *aggregation process* groups the radiation sources of different centers in the child level into a single center at the parent level and let the interaction of radiation sources between two far-away groups to be proceeded through outer multipole expansions [12]. The *translation process* translates the coefficients of outer multipole expansions between the second nearby centers (second nearby centers will be explained later) in the same level to proceed the interaction of radiation sources. The *disaggregation process* distributes the translated coefficients of multipole expansions of the centers in parent levels to those of the centers in child levels. To be more specific, in this three-level case, the aggregation process includes to group sources of the basis function into the centers "$\cdot$" in level 3 and group sources of four centers "$\cdot$" in the level 3 into a single center "o" in level 2. The translation process includes the translation of coefficients of outer multipole expansions from each center "$\cdot$" to the second nearby center "$\cdot$" in level 3 and from each center "o" to the second-nearby center "o" in level 2; the disaggregation process includes to distribute translated coefficients from the center "o" in level 2 to the center "$\cdot$" in level 3 and from the center "$\cdot$" in level 3 to original unknowns.

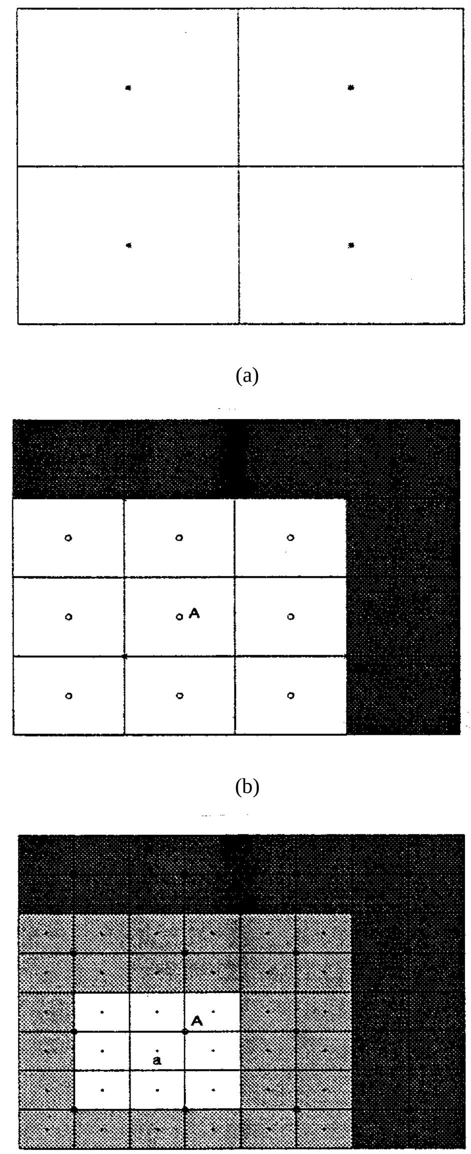

(a)

(b)

(c)

Fig. 2. A three-level MLFMA. (a) Level 1. (b) Level 2. (c) Level 3.

It is easy to understand that either aggregation process or disaggregation process requires only $O(N)$ computer operations in each level. For instance, consider the level–3 aggregation process. Suppose the number of the unknowns in each square in this level is N_3, hence, there are $M = N/N_3$ subsquares. Since the number of the computer operation in each subsquare is equal to the number of the outer multipole expansions [12], which approximates to N_3, therefore, the computer operation of the total level-3 aggregation process is $N_3 \times M = N$. It should be noted that the problem of different numbers of outer multiple expansions in different levels is solved by interpolation and anterpolation techniques for the aggregation process and the disaggregation process, respectively [13]. Since interpolation matrices and anterpolation matrices are sparse, the total computer operation for these process is $O(N)$ in each level.

Next, let us consider the translation process, which is the essential process resulting in the reduction of the computational complexity of the MLFMA. To understand the translation process in the MLFMA, we first define *second nearby centers*, which are not nearby centers in the child level, but is nearby center in the parent level. For example, in level 3, the centers in the lightly shaded squares are the second nearby centers of the center "a," others are not. Hence, the number of the second nearby centers is less than a constant C, which can be evaluated as 27 in this case. In the MLFMA, the translation of coefficients of outer multipole expansions just proceeds in second nearby centers because the interaction between further source centers have been proceeded in the parent level. For example, the coefficients of the outer multipole expansions need to be translated to the center "a" in level 3 are those in the lightly shaded squares, whereas the action from the centers in the darkly shaded squares to the center "a" is obtained by disaggregation of the coefficients of the outer multipole expansions in the center "A," which is obtained from the parent level translation process. The crucial point in the MLFMA is that the computer operation of this translation process in each level is still $O(N)$, which is achieved by the diagonal technique through using plane wave basis, namely, the translation of N_l coefficients of outer multipole expansions from one center to another second nearby center requires $O(N_l)$ computer operations not $O(N_l^2)$. Consider the level-3 translation process since the number of the outer multipole expansions for each subsquare, which approximates to N_3, is the number of the computer operation in the translation process between two subsquares, the computer operation of the translation process in this level approximates to $C \times N_3 \times M = C \times N$. Because the computer operation of the aggregation process, translation process and disaggregation process in each level are all $O(N)$ and there are $\log(N)$ level, the computer operation of the matrix-vector multiplication is $O(N \log N)$. Since the interpolation (anterpolation) matrices are the same for different groups in the same level, the total memory requirement is, hence, $O(N)$.

IV. Results

A general code (FA-FE-BI) of the fast and accurate FE-BI technique with the inward-looking preconditioner has been developed for scattering by a large body with cracks and cavities. In this code, the *bicubic interpolation* [17] is employed in the MLFMA implementation for the problem of different numbers of outer multiple expansions in different levels. The integral over a unit sphere in the second elementary identity in the fast multipole method (FMM) is evaluated with Gaussian quadrature method mentioned in [12].

In this section, we present representative numerical results of five examples obtained with the FAFEBI code to demonstrate the accuracy, efficiency and capability of this technique. The aim of the first four experiments is to demonstrate the accuracy and validity of this technique. Initially, the method of moments (MoM) is used to calculate the scattering by a conducting body without cracks. Then the MoM and FA-FE-BI are used to calculate the scattering by the same body but with a empty crack. Hence, the results from these two different techniques can be compared to demonstrate the accuracy and validity of the

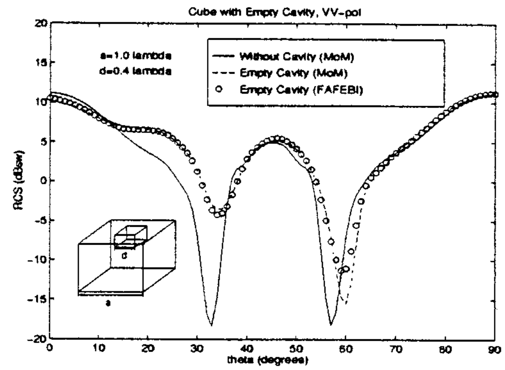

(a)

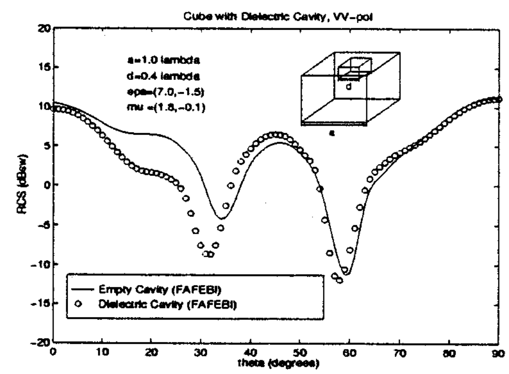

(b)

Fig. 3. Monostatic RCS of a conducting cube with a cavity in the E-plane. (a) Empty cavity. (b) Dielectric cavity.

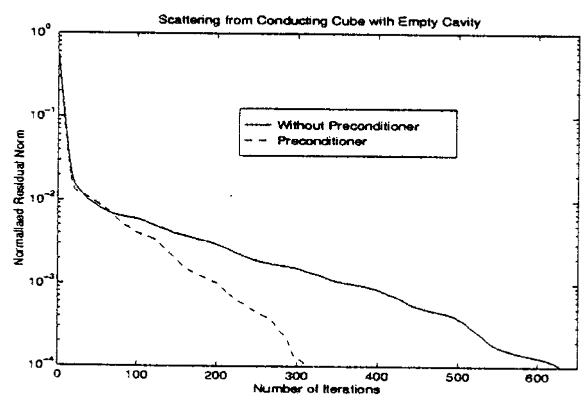

Fig. 4. Comparison of the rate of convergence between with the preconditioner and without the preconditioner.

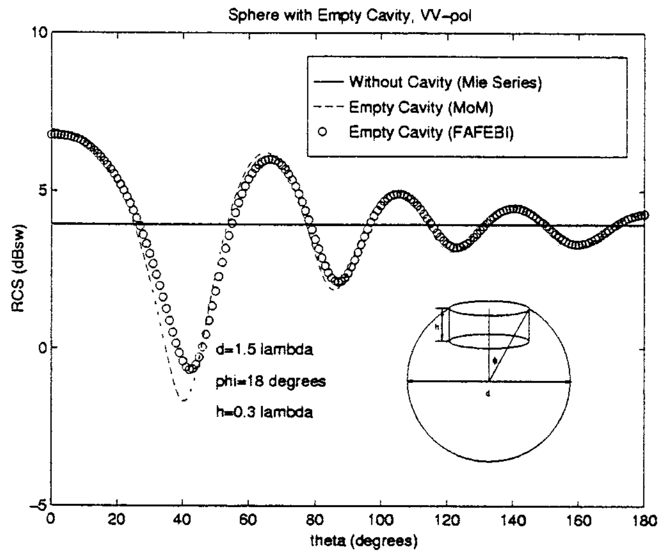

(a)

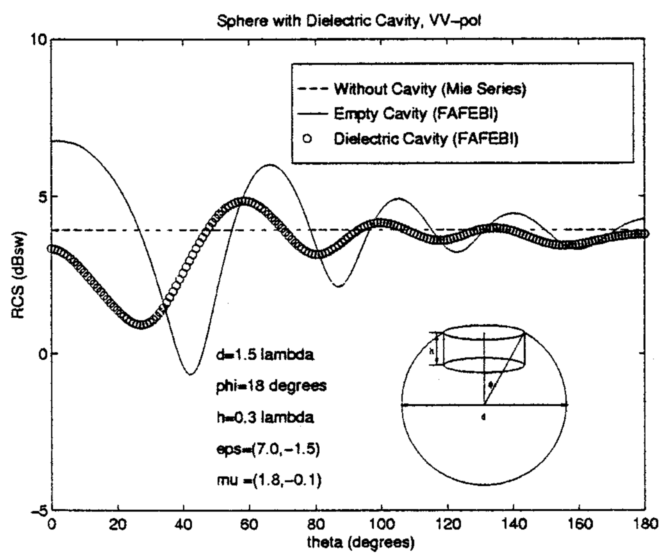

(b)

Fig. 5. Monostatic RCS of a conducting sphere with a cavity in the E-plane. (a) Empty cavity. (b) Dielectric cavity.

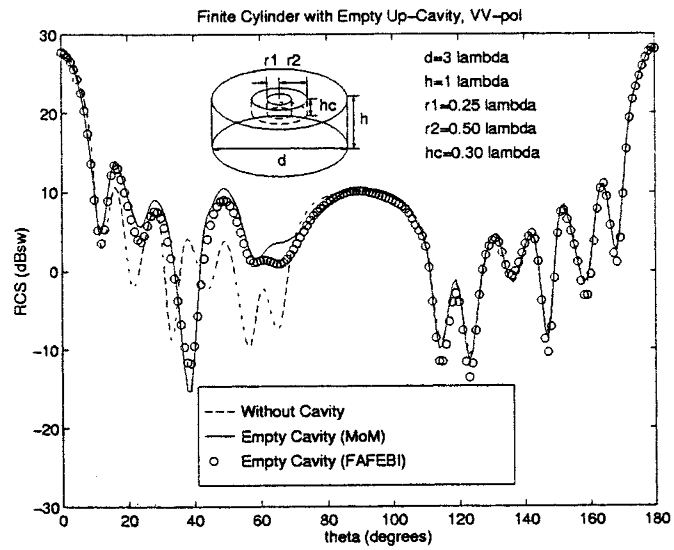

(a)

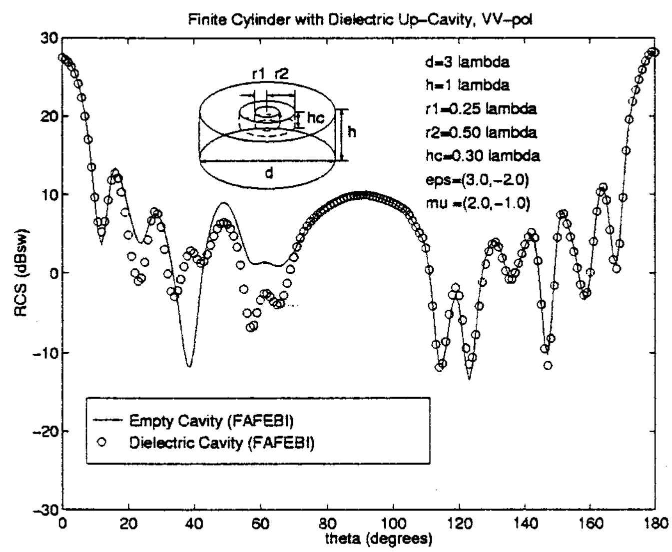

(b)

Fig. 6. Monostatic RCS of a conducting cylinder with a ring-like crack in the E-plane. (a) Empty cavity. (b) Dielectric cavity.

FA-FE-BI code and also get some insights of the effect of cracks and cavities to the scattering behavior. At last, the FA-FE-BI is used to compute the scattering by the same body with the same cracks filled with lossy materials, which is not readily available by the MoM technique. After these four numerical experiments sufficiently confirming the accuracy and validity of this technique, a large problem is analyzed to demonstrate the efficiency and capability of this technique.

The first example is the scattering by a conducting cube with a cavity illustrated in Fig. 3. Fig. 3(a) presents the comparisons between the numerical results from the FA-FE-BI and the MoM for the cube with a cavity and those from the MoM for the same cube without cavities. We can observe the effect of the cavity to the radar cross section (RCS) and good numerical agreements between these two different techniques. Fig. 3(b) demonstrates the effect of lossy materials to the RCS. Comparison of the rate of convergence between with the preconditioner and without the preconditioner is given in Fig. 4, demonstrating that the rate of convergence with the preconditioner is about twice faster than that without the preconditioner.

The second example is the scattering by a conducting sphere with a cylindrical cavity. This example differs from the first one in that the cavity is situated on a curved surface. Fig. 5(a) presents the comparisons between the numerical results from FA-FE-BI and MoM for the sphere with a empty cavity and those from MoM for the same sphere without cavities. As expected, the cavity in this example has much more effect on the RCS than that in the first example. Again, good numerical agreement is obtained between these two techniques, demonstrating the accuracy and validity of the FA-FE-BI technique.

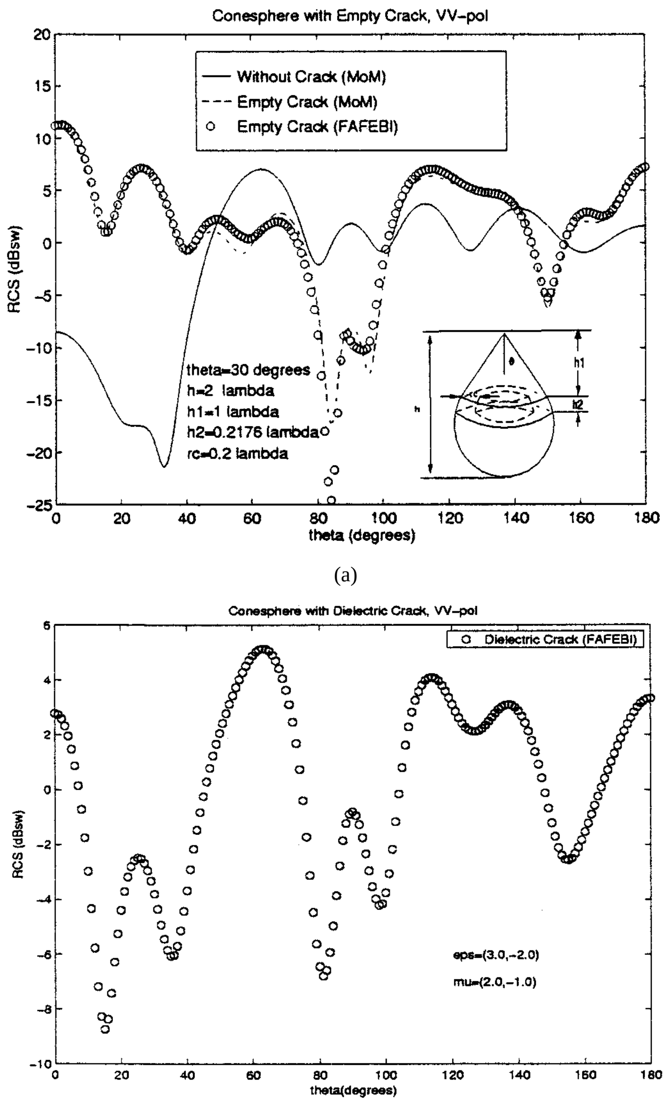

(a)

(b)

Fig. 7. Monostatic RCS of a conducting conesphere with a crack in the E-plane. (a) Empty cavity. (b) Dielectric cavity.

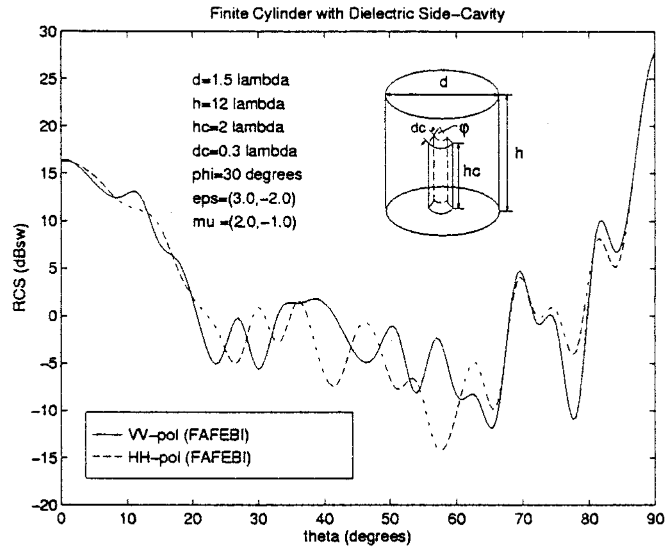

Fig. 8. Monostatic RCS of a conducting cylinder with a crack.

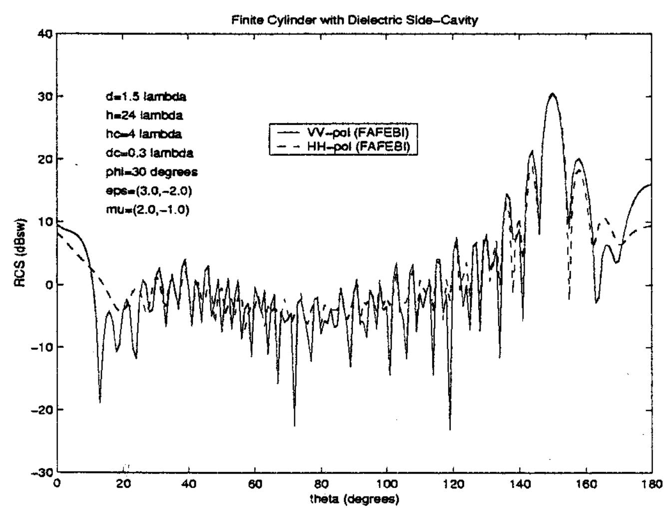

Fig. 9. Bistatic RCS of a 24-wavelength conducting cylinder with a crack at the incident angle $\theta = 30°$, $\varphi = 0°$.

Fig. 5(b) presents the RCS by the same sphere with the same cavity but filled with lossy materials having $\epsilon_r = (3.0, -2.0)$ and $\mu_r = (2.0, -1.0)$.

Next, two more complex examples are presented. They are the scattering by a conducting cylinder with a ring-like crack and the scattering by a conducting conesphere with a crack. Figs. 6 and 7 present numerical results of the monostatic RCS, showing that the cracks greatly affect the RCS, especially for conducting conesphere where the crack completely changes the RCS pattern. This shows that strong and complex interactions exist between the crack and the conesphere. The FA-FE-BI and MoM again give a fairly good numerical agreement.

At last, we compute the scattering by a conducting cylinder having $1.5\ \lambda_0$ diameter and $12\ \lambda_0$ height, on the side of which there is a lossy-material-filled crack having $2\ \lambda_0$ long, $0.3\ \lambda_0$ deep, and 30° subtented angle. Fig. 8 presents the both vertical (VV) polarization and horizontal (HH) polarization monostatic RCS. Fig. 9 is the bistatic RCS by a more large conducting cylinder with $24\ \lambda_0$ height and $4\ \lambda_0$ long crack (other dimensions are the same as those in Fig. 8) at the incident angle $\theta = 30°$, $\phi = 0°$.

For all of the above calculations, the number of multipoles for truncating the expansion in the addition theorem is chosen as $L = kd + 2\ln(kd + \pi)$ (d is the distance between two group centers). The computation is performed at the DEC alpha workstation with 50 Mflops and 128M RAM. The memory requirement and CPU time for all examples are listed in Table I from which we can see that the MLFMA with preconditioner significantly reduce the memory requirement and CPU time.

V. Conclusion

In this paper, the fast and accurate FE-BI formulation has been applied to analyze the problem of scattering by a large body with cracks and cavities. A thorough analysis on the cost

TABLE I
THE MEMORY REQUIREMENT AND CPU TIME OF COMPUTATION OF ONE MONONSTATIC RCS BY VARIOUS SCATTERS WITH A LOSSY MATERIAL FILLED CRACK

Scatterers	MLFMA+Preconditioner			Without MLFMA+Preconditioner	
	Level of MLFMA	Memory (Mb)	CPU (s)	Memory (Mb)	CPU (s)
brick	2	14.1	43	52.3	650
sphere	3	12.3	54	117.4	1206
cylinder in Fig.6	4	23.3	219	587.1	
conesphere	3	13.8	56	66.8	506
cylinder in Fig.8	6	50.6	571	3109.4	
cylinder in Fig.9	7	97.1	1107	11578.0	

of this technique clearly demonstrates that it has computational complexity $O(N \log N)$ and memory requirement $O(N)$. An inward-looking approach has been successfully employed as a preconditioner to speed up the rate of convergence of the CG solver. A variety of numerical examples are presented, demonstrating that the scattering problem investigated in this paper can be generally, accurately, efficiently computed by this technique.

REFERENCES

[1] M. I. Herman and J. L. Volakis, "High frequency scattering by a resistive strip and extensions to conductive and impedance strips," *Radio Sci.*, vol. 22, no. 3, pp. 335–349, 1987.

[2] T. B. A. Senior and J. L. Volakis, "Scattering by gaps and cracks," *IEEE Trans. Antennas Propagat.*, vol. 37, pp. 744–750, June 1989.

[3] A. K. Dominek, H. T. Shamansky, and N. Wang, "Scattering from three-dimensional cracks," *IEEE Trans. Antennas Propagat.*, vol. 37, pp. 586–591, May 1989.

[4] J. M. Jin and J. L. Volakis, "A finite element-boundary integral formulation for scattering by three-dimensional cavity-backed apertures," *IEEE Trans. Antennas Propagat.*, vol. 39, pp. 97–103, Jan. 1991.

[5] ——, "A hybrid finite element method for scattering and radiation by microstrip patch antennas and arrays residing in a cavity," *IEEE Trans. Antennas Propagat.*, vol. 39, pp. 1598–1604, Nov. 1991.

[6] N. Lu and J. M. Jin, "Application of fast multipole method to finite-element boundary-integral solution of scattering problems," *IEEE Trans. Antennas Propagat.*, vol. 44, pp. 781–786, June 1996.

[7] J. M. Jin, S. S. Ni, and S. W. Lee, "Hybridization of SBR and FEM for scattering by large bodies with cracks and cavities," *IEEE Trans. Antennas Propagat.*, vol. 43, pp. 1130–1139, Oct. 1995.

[8] A. D. Greenwood, S. S. Ni, J. M. Jin, and S. W. Lee, "Hybridization of SBR/FEM method to compute radiation pattern from a microstrip patch antenna in a complex geometry," *Microwave Opt. Tech. Lett.*, vol. 13, pp. 84–87, Oct. 1996.

[9] X. Q. Sheng, J. M. Jin, J. M. Song, C. C. Lu, and W. C. Chew, "On the formulation of hybrid finite-element and boundary-integral method for 3-D scattering," *IEEE Trans. Antennas Propagat.*, vol. 46, pp. 303–311, Mar. 1998.

[10] A. F. Peterson, "Analysis of heterogeneous electromagnetic scatterers: Research progress of the past decade," *Proc. IEEE*, vol. 79, pp. 1431–1441, Oct. 1991.

[11] J. M. Jin, *The Finite Element Method in Electromagnetics*. New York: Wiley, 1993.

[12] R. Coifman, V. Rokhlin, and S. Wandzura, "The fast multipole method for the wave equation: A pedestrian prescription," *IEEE Trans. Antennas Propagat. Mag.*, vol. 35, pp. 7–12, June 1993.

[13] J. M. Song and W. C. Chew, "Multilevel fast-multipole algorithm for solving combined field integral equations of electromagnetic scattering," *Microwave Opt. Tech. Lett.*, vol. 10, no. 1, pp. 14–19, Sept. 1995.

[14] J. M. Song, C. C. Lu, and W. C. Chew, "MLFMA for electromagnetic scattering by large complex objects," *IEEE Trans. Antennas Propagat.*, vol. 45, pp. 1488–1493, Oct. 1997.

[15] A. J. Poggio and E. K. Miller, "Integral equation solutions of three dimensional scattering problems," in *Computer Techniques for Electromagnetics*. Oxford, U.K.: Permagon, 1973, ch. 4.

[16] S. M. Rao, D. R. Wilton, and A. W. Glisson, "Electromagnetic scattering by surfaces of arbitrary shape," *IEEE Trans. Antennas Propagat.*, vol. AP-30, pp. 409–418, May 1982.

[17] W. H. Press, S. A. Teukolsky, W. T. Vetterling, and B. P. Flannery, *Numerical Recipes in Fortran*. New York: Cambridge Univ. Press, 1992.

Xin-Qing Sheng was born in Anhui, China, in 1968. He received the B.S., M.S., and Ph.D. degrees from the University of Science and Technology of China (USTC), Hefei, China, in 1991, 1994, and 1996, respectively.

From 1994 to 1996, he was a Research Assistant in the Department of Electronic Engineering and Information Science, USTC, where he developed a code of hybridization of the finite-element method and mode-matching method for discontinuity problems in waveguides. From 1996 to 1998, he worked in the Center for Computational Electromagnetics, Department of Electrical and Computer Engineering, University of Illinois at Urbana-Champaign, where he developed a code of the hybrid FEM/MLFMA for large coated bodies. Since 1998 he has been with the City University of Hong Kong as a Research Fellow, where he is currently supervising several projects. His research interests focus on computational electromagnetics covering computer solutions of scattering, radiation and transmission problems, computing algorithms, and application of achievement in mathematics and computer science.

Edward Kai-Ning Yung received the B.Sc. (electrical engineering, with special distinction), M.Sc., and Ph.D. degrees in 1972, 1974, and 1977, respectively, all from the University of Mississippi.

After graduation, he was briefly with the Electromagnetic Laboratory, University of Illinois at Urbana-Champaign. He returned to Hong Kong in 1978 and began his teaching career at the Hong Kong Polytechnic. He joined the newly established City University of Hong Kong in 1984 and was instrumental in setting up a new department. He was promoted to Full Professor in 1989 and, in 1994, he was awarded one of the first two personal chairs in the University. He is the Founding Director of the Wireless Communications Research Center, formerly known as Telecommunications Research Center. Currently, he heads the Department of Electronic Engineering, the largest of its kind in Hong Kong with 220 full-time staff members, including 65 faculty members. He is the Principal Investigator of many funded projects. He is the External Examiner of many graduate students in sister universities, both local and overseas, and holds honorary professorships in two universities in China. He is the author or coauthor of over 100 articles in journals and has presented equally as many papers at international conferences. He is also active in applied research, consultancy, and other types of technology transfers. He holds one patent. He remains active in research in microwave devices and antenna designs for wireless communications.

Dr. Yung shared (with his colleagues) the Young Scientist Award in the International Symposium on Antennas and Propagation in Tokyo in 1996. He was the recipient of many awards in applied research, including the Grand Prize in the Texas Instrument Design Championship in 1991, the Silver Medal in the Chinese International Invention Exposition in 1998, and the CMA Design Award in 1999. Currently, he is the Vice President of the Hong Kong Institution of Engineers. Over the years, he has been elected President of the Hong Knog Association for the Advancement of Science and Technology (1998–1999), President of the Association of Experts for the Modernization of China (1989–1990 and 1998–1999), and Chairman of the Electronics Division, Hong Kong Institution of Engineers. He has been the General Chairman of many international conferences held in Hong Kong. He is a Fellow of the Chinese Institution of Electronics, the Institute of Electrical Engineers (U.K.) and the Hong Kong Institution of Engineers. He is a member of Eta Kappa Nu, Phi Kappa Phi, Tau Beta Pi, and the Electromagnetics Academy. He is listed in the *Who's Who in the World* and *Who's Who in the Science and Engineering in the World*.

Chi H. Chan received the Ph.D. degree in electrical engineering from the University of Illinois at Urbana-Champaign, in 1987.

He joined the Department of Electronic Engineering at the City University of Hong Kong in April 1996 as a Professor and was promoted to Professor (Chair) of Electronic Engineering in 1998. He has been an Associate Dean (Research) of Faculty of Science and Engineering at City University of Hong Kong since 1998. He is a Guest Professor of Xik'an Jiaotong University. His research focuses on computational electromagnetics and wireless communications. He is the author of *MULTFSS*, a general-purpose frequency-selective surface analysis code currently distributed by DEMACO, Inc., Champaign, IL as part of its McFSS package.

Professor Chan was a recipient of the 1991 U.S. National Science Foundation Presidential Young Investigator Award. He is a Fellow of the Chinese Institute of Electronics (CIE) and the Institute of Electrical Engineers (IEE).

J. M. Jin, photograph and biography not available at time of publication.

W. C. Chew, photograph and biography not available at time of publication.